Gyrokinetic theory and simulation of momentum transport and energy exchange

R. E. Waltz,

Work with: G.M. Staebler and J. Candy

General Atomics

PPPL Theory/NSTX Seminar

October 22, 2007

Abstract

A synopsis of physics results from GYRO gyrokinetic simulations from the last five years will be given with a brief review. The focus however is on new theory and simulation of the ExB shear and coriolis angular momentum pinch effects needed to understand the intrinsic toroidal rotation in tokamaks without external torque in the core. In addition, new theory and simulations showing that turbulent heating is dominantly an electron-ion energy exchange is presented.

Outline

- Five year synopsis of GYRO physics results

  _Bohm scaled DIII-D L-modes and gyroBohm scaled H-modes

- Momentum transport

  _Heuristic description of intrinsic toroidal rotation and momentum pinches

  _GYRO verification of ExB shear pinch and finite parallel velocity pinch

  _Gyrokinetic formulation of toroidal angular momentum transport and poloidal rotation

- Turbulent Energy Exchange

Five year synopsis of GYRO physics results

GYRO[Candy 2003a] publications demonstrating:

[2002]

* Bohm to gyroBohm transition at decreasing rho-star in global gyrokinetic ITG- adiabatic electron simulations [Waltz 2002].

[2003]

* Bohm scaling in physically realistic+ gyrokinetic simulations of DIII-D L-mode rho-star pair matching transport within error bars on ion temperature gradients[Candy 2003b]

+(ITG ions and finite-beta and collisional electron physics with real shaped geometry, profile ExB shear, experimental profiles, etc)

[2004]

* small turbulent dynamo in tokamak current-voltage relation[Hinton 2004]
* local gyrobohm flux simulations to be vanishing rho-star limit of global simulations [Candy 2004].
• transport is smooth across minimum-q surface [Candy 2004b]

[2005]

* global gyrokinetic transport solutions, i.e. predicted temperature and density profiles from balance of transport and source flows [Waltz 2005a].
* electron temperature gradient drives plasma flow pinches and recovered the D-V description of experimental Helium transport studies[Estrada-Mila 2005].
* weak beta scaling of transport up to about half the MHD beta limit [Candy 2005]
* turbulence draining from unstable radii and spreading to stable radii providing a heuristic model of non-local transport [Waltz 2005b,Waltz 2005c].

Synopsis (cont'd)

[2006]

* connection between velocity space resolution, entropy saturation and conservation, and numerical dissipation [Candy 2006a].

*** perfectly projected experimental profiles in rho-star gyroBohm-like DIII-D H-modes to Bohm-scaled local diffusivity while simulation of actual profiles showed gyroBohm scaling and match transport within error bars. Perfectly project Bohm-like DIII-D L-mode simulations remained Bohm [Waltz 2006a]**

* profile corrugations at low-order rational surfaces observed in DIII-D minimum q=2 discharges providing an ExB shear layer to initiate a transport barrier [Waltz 2006b].

* that including so-called parallel nonlinearity has no effect on simulated energy transport at rho_stars less than one percent [Candy 200b]

* density peaking from plasma pinch in DIII-D L-mode simulations with actual collisionality[Estrada-Mila 2006b].

* first simulation of fusion hot alpha transport from ITG/TEM micro-turbulence found to be small with ITER parameters [Estrada-Mila 2006b].

Synopsis (cont'd)

[2007]

* ETG simulations with kinetic ion cures unphysically large saturation levels in conventional ETG simulations with adiabatic ions [Candy 2006c, Candy 2007]

* high-Reynolds number coupled ITG/TEM-ETG simulations (at close to physical ion to electron mass ratio) show low-k ITG/TEM and high-k ETG transport decoupled when both strongly driven but ITG/TEM can drive ETG transport in ETG stable plasmas; high-k spectrum tends to be isotropic [Waltz 2007a]

* 400+ web parameter scan database of flux tube simulations used to fit nonlinear saturation rule with ExB shear stabilization in TGLF [Staebler 2005, Staebler 2007] theory based transport code model [Kinsey 2005, Kinsey 2006, Kinsey 2007]

* angular momentum pinch from ExB shear and pinch from "coriolis" force important for understanding experiments with intrinsic toroidal rotation; turbulent shift from neoclassical poloidal rotation is small [submitted to Phys. Plasmas, waltz 2007b]

* radially integrated turbulent ohmic heating from parallel and drift currents is actually close to an electron-ion energy exchange and small compared to energy transport flow [submitted , Waltz 2007c]

Bohm scaled DIII-D L-modes and gyroBohm scaled H-modes

- Experiments to determine the local rho-star scaling of diffusivity require rho-star pairs to have "nearly perfect dimensional similarity" which is very difficult.

- Because the rho-star variation is only 1.6x, the Bohm vs gyroBohm difference in measured temperatures is only 17%, barely outside the error bars

- GYRO simulations provide an important analysis of experimental imperfection and uncertainty by simulating rho-star pairs directly and in comparison to simulations of "perfectly projected rho-star pairs"

- L-modes are typically Bohm-scaled (why?) and H-modes typically (but not always) are gyroBohm scaled, yet (for DIII-D) the H-mode pairs have larger rho-star….shouldn't they have more tendency to Bohm-scaling?

- GYRO simulations can clarify the mechanism breaking gyroBohm scaling:
  <u>local</u> profile shearing or <u>non-local</u> turbulent draining-spreading ?

GYRO DIII-D experimental analysis of ρ*-scaling pairs: Mechanisms for breaking gyroBohm scaling to Bohm scaling

$$rho\_star: \ \rho_* \equiv \rho_s / a < 1\%, \quad \rho_s \equiv c_s/\Omega$$

$$gyroBohm: \ \chi_{gB} = [c_s/a]\rho_s^2 = [c_s\rho_s]\rho_* = \chi_B \rho_*$$

$$Bohm: \ \chi_B \equiv [c_s\rho_s] = \chi_{gB}/\rho_*$$

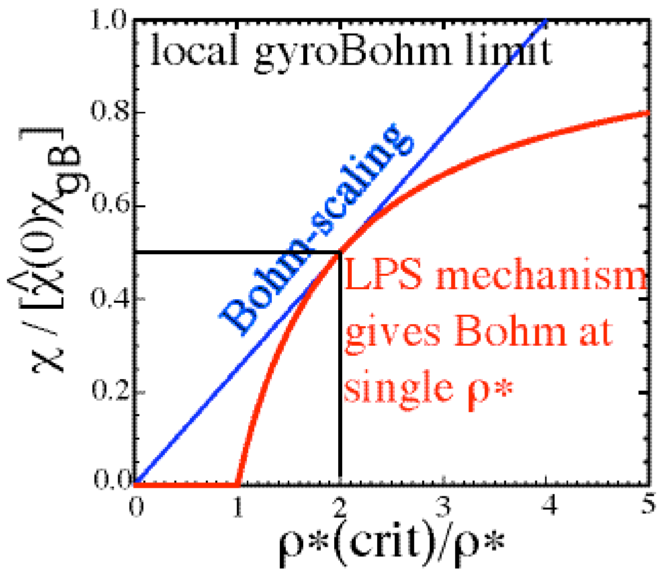

- Tokamak transport gyroBohm sized and Bohm scaling should theoretically extrapolate to gyroBohm scaling
- Local profile shearing (LPS)[Garbet&Waltz (1996)]: similar to local ExB shear stabilization

$$\chi = \hat{\chi}(0)\chi_{gB}[1 - \rho_*/\rho_*(crit)]$$ minus = stabilization

- Nonlocal turbulence spreading (NTS) [Lin,Hahm,et al (200_,_].

$$\chi = \hat{\chi}(0)\chi_{gB}[1 - \rho_*/\rho_*(crit)]$$ (big χ) Bohm in unstable "draining" region like LPS

$$\chi = \hat{\chi}(0)\chi_{gB}[1 + \rho_*/\rho_*(crit)]$$ (small χ) "super-gyroBohm" in stable "spreading" region

- Empirical "Mixed Bohm-gyroBohm Model" separate mechanisms……. Extrapolates to ITER Bohm scaling at very small ρ*

$$\chi = \hat{\chi}(0)\chi_B[\rho_*(crit) + \rho_*]$$

GYRO DIII-D experimental analysis of ρ*-scaling pairs: L-mode pair has Bohm scaling with good profile similarity

- **A ρ*-scaling experiment is a power scaling to match a dimensionally similar temperature profile. For a ρ* =0.0025 - 0.004 pair, the difference between Bohm and gyroBohm is just outside temperature error bars of 9%. Accuracy of profile similarity crucial particularly with stiff core.**

- **Perfect profile similarity can be obtained by projecting data:**
  B α $1/(\rho^*)^{3/2}$, $T_0(r)$ α $1/\rho^*$, $n_0(r)$ α $1/\rho^*$, $v_{\phi 0}(r)$ α $1/(\rho^*)^{1/2}$, $\phi_0(r)$ α $1/\rho^*$

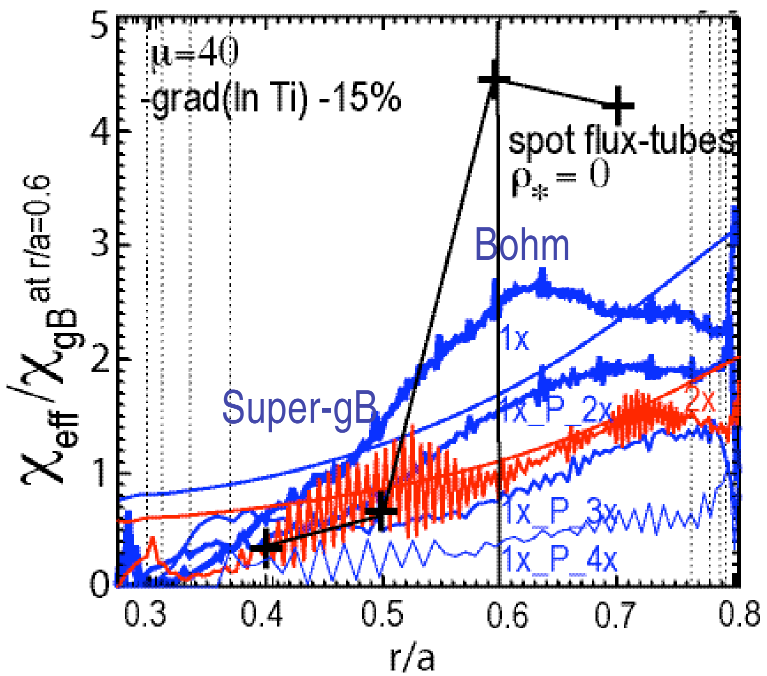

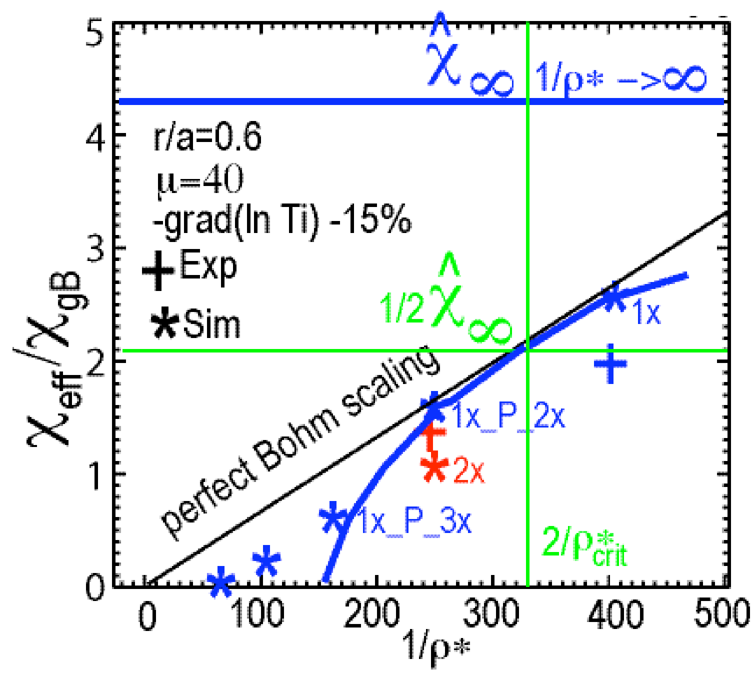

1x => ρ*=0.0025
2x, 2x => ρ*=0.0040
3x => ρ*=0.0006
4x => ρ*=0.0004

- **Evidence of super-gyroBohm in stable (or less unstable) inner core suggests NTS is dominant here.**

GYRO DIII-D experimental analysis of ρ*-scaling pairs: L-mode ρ*- projected data and sensitivity to grad-Ti and ExB shear

- DIII-D core is very “stiff” and strong ExB shear (high toroidal rotation) accounts for much of the good confinement.

- GYRO simulations match experiments with 15% reduction of -grad[lnT] or 15% increase in ExB shear: Reduces 2-fold larger transport to well within experimental error bars.

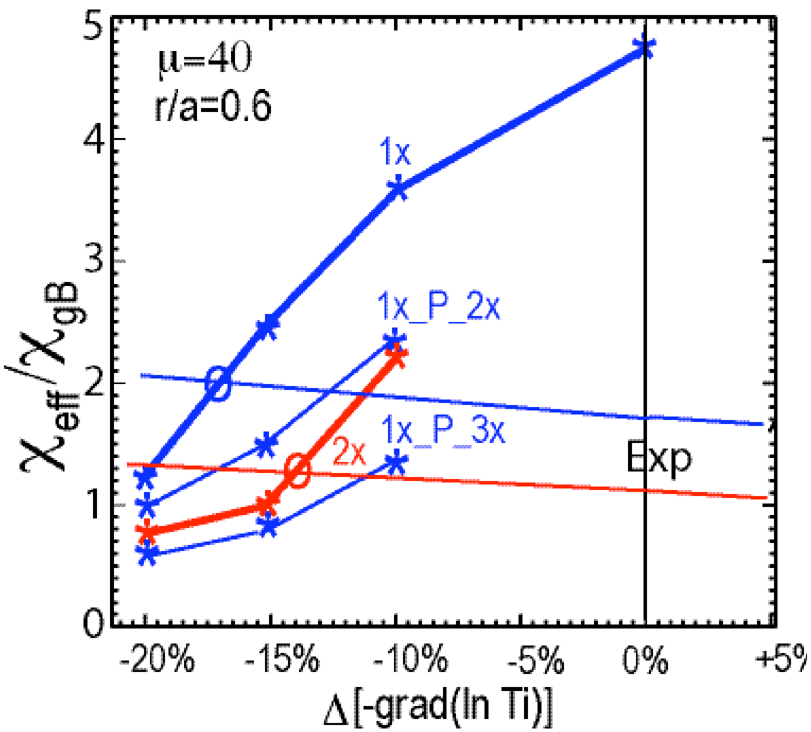

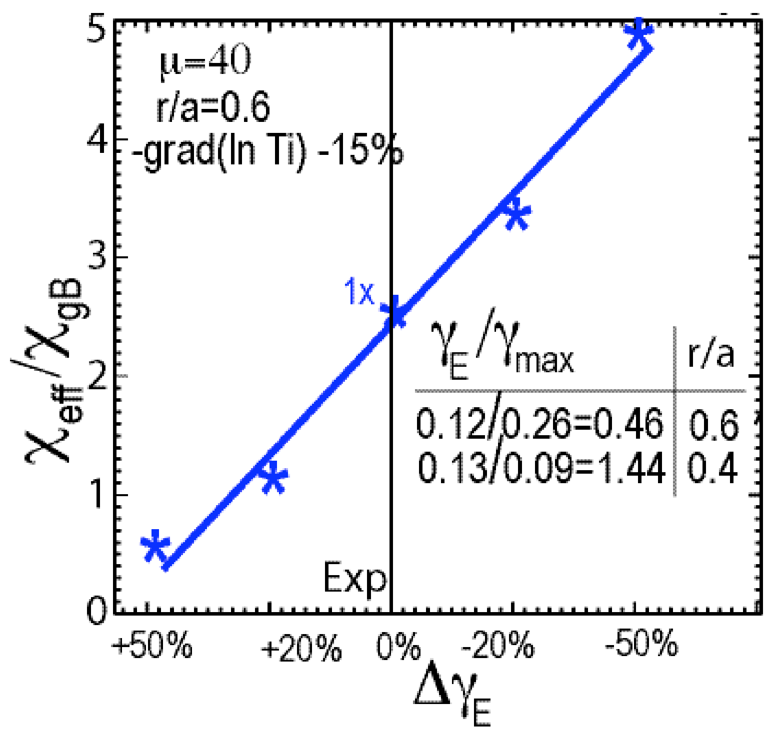

GYRO DIII-D experimental analysis of ρ*-scaling pairs :
H-mode larger ρ*- pair measured gyroBohm with poor similarity

- **Puzzle: Going from Bohm L-mode ρ*=0.0025-0.004 to H-mode at larger ρ*=0.004-0.006 EXPECT more Bohm NOT gyroBohm ?**

- **GYRO simulations match experiments (with 15% reduction) with actual H-mode data and show gyroBohm scaling(1x vs 2x);**
….but projected data with perfect similarity show Bohm (1x vs 1x_P_2x).

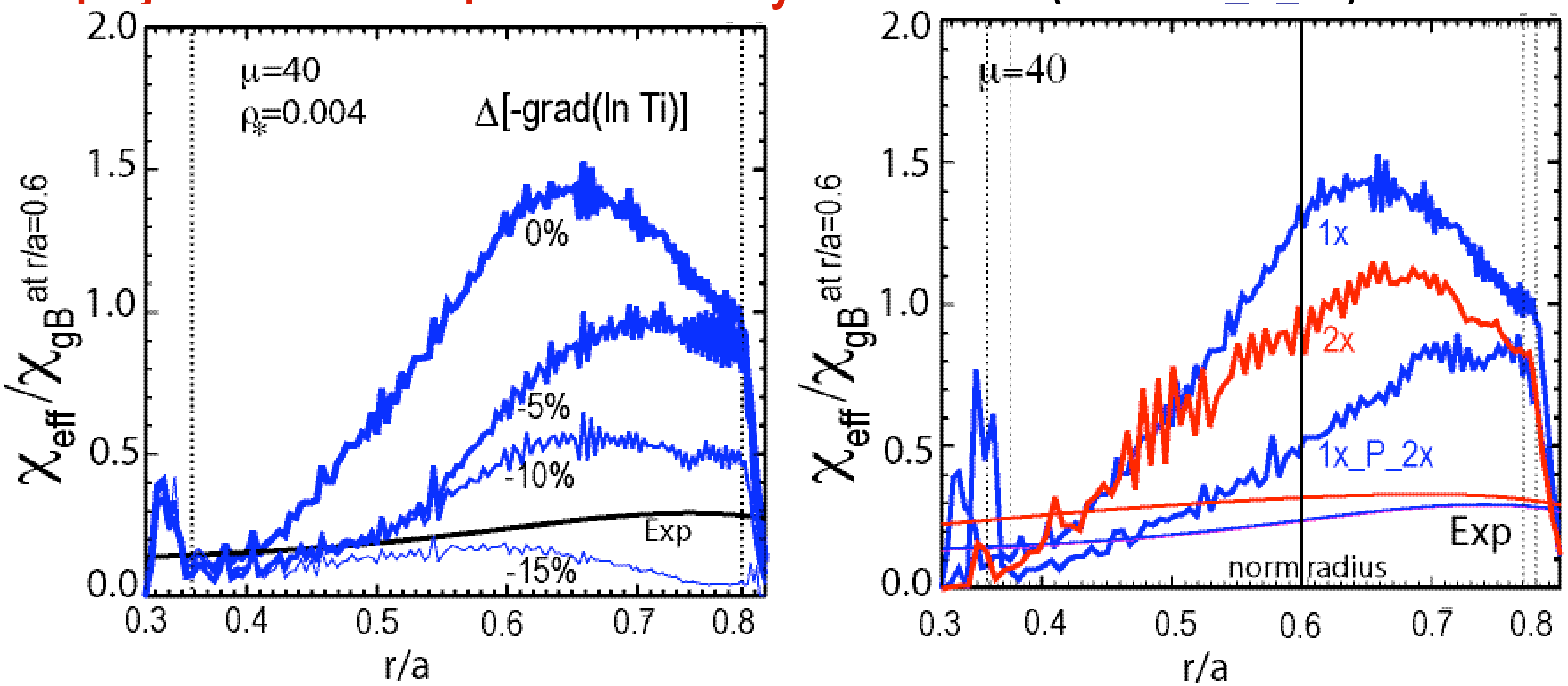

1x => ρ*=0.004 ; 2x => ρ*=0.006

Summary: Bohm scaled DIII-D L-modes and gyroBohm scaled H-modes

- GYRO can match DIII-D L- and H-mode transport with 15% smaller -grad[lnTi] or larger ExB shear.

- The DIII-D L-mode rho-star pair has excellent similarity conditions and GYRO simulations of perfectly projected rho-star pair verifies Bohm scaling.

- The DIII-D H-mode “gyroBohm scaled” rho-star pair (with 50% larger rho-stars) has poor similarity and GYRO simulations of perfectly projected rho-star pair has Bohm scaling

- If the global simulation diffusivity is 1/2 the local flux-tube value, then have idealized Bohm scaling.

- Nonlocal turbulent draining from unstable regions (Bohm - decrease) and spreading to more stable regions (super-gyroBohm -increase) apparent. Local profile shearing is weak.

Momentum Transport

Heuristic description of intrinsic toroidal rotation

- Toroidal momentum continuity equation:

$$\partial[nv_\phi]/\partial t + r^{-1}\partial[r\Gamma_x^\phi]/\partial r = S_\phi(r)$$

Actually we need to consider the flux surface average of toroidal angular momentum (TAM) continuity $m_i\langle Rnv_\phi\rangle$, but such details are suppressed here.

- TAM is a conserved quantity. For intrinsic toroidal rotation with no internal sources, $S_\phi(r)=0[r=0:a]$ the "source" of the momentum is in the banana orbit loses at the edge $S_\phi(r)>0[r=a:a+\rho_{bananna}]$

- At steady state: $\Gamma_x^\phi(r)=(a/r)\Gamma_x^\phi(a)$

At some earlier time $\Gamma_x^\phi(a)<0$ and toroidal angular momentum flowed into the core r< a until it starts to flow out $\Gamma_x^\phi(a)>0$. The edge is both a source and sink (wall neutral CEX). At steady state $\Gamma_x^\phi(a)\sim 0$, we are looking for the *existence of a null transport flow state:* $\Gamma_x^\phi(r)=0[r=0:a]$ with finite values of v_ϕ and $\partial v_\phi(r)/\partial r$.

- In the DIIID case $v_\phi(a)\sim 0$ and $v_\phi(r)$ peaked near r~a/2 [i.e. $\partial v_\phi(a/2)/\partial r\sim 0$]

Heuristic description (cont'd)

- Descriptive (heuristic) transport flow model verified by GYRO simulations:

$$\Gamma_x^{\phi}(r) \equiv -n\eta_{\phi}^{eff}\,\partial v_{\phi}/\partial r \equiv -n\eta_{\parallel}^{eff}\,\partial v_{\parallel}/\partial r$$
$$= -n\eta_{\parallel}\partial v_{\parallel}/\partial r - n(\eta_{v}/a)v_{\parallel} - n\eta_{E}\partial v_{ExB}/\partial r + v_{\phi}\Gamma_x$$

At steady state, the core (even with peaked density profile) will be in "null" plasma flow state $\Gamma_x \sim 0$ and positive only close to edge recycling.
[In any case we ignore convection here.]

$$v_{\parallel} = (B_t/B)v_{\phi} + (B_p/B)v_{\theta}$$
$$v_{ExB} = -v_{*}[\nabla p_i] + (B_t/B)v_{\theta} - (B_p/B)v_{\phi}$$
$$v_{\theta} = v_{*}^{neo} = -K^{neo}c_s\rho_{*}a\,\partial \ln T_i/\partial r$$

- In toroidal geometry finite $v_{\parallel}$ terms in the curvature drifts

A. G. Peeters, C. Angioni, D. Strintzi, "The toroidal momentum pinch velocity" PRL 2007,

show $(\eta_{v}/a) > 0$ in an ITG adiabatic electron quasilinear model allowing a pinched $\Gamma_x^{\phi}(r) = 0$ state with $-[\partial v_{\parallel}/\partial r]/v_{\parallel} > 0$ so called "coriolis pinch"

Heuristic description (cont'd)

- In slab geometry (and now GYRO verified in toroidal geometry)

R.R. Dominguez and G.M. Staebler, Phys. Fluids B5 (1993) 3876

showed with an ITG-TEM quasilinear model how ExB shear (η_E -term) can allow null $\Gamma_x^\phi \sim 0$ flow states and

[G.M. Staebler et al, BAPS 46 (2001) p221-LP1 17], "Heating Induced Toroidal Rotation and Other Consequences of Anomalous Momentum transport"
argued

"spontaneous toroidal rotation during heating without external torque was shown to follow from the off diagonal nature of the toroidal viscous stress"

[G.M. Staebler TTF 2001 poster]

Note the "stress" $\Pi_{x\phi} \propto \Gamma_x^\phi$ is essentially same as radial flow of toroidal momentum.

Heuristic: How does intrinsic toroidal rotation result?

- Set $(\eta_\upsilon/a)=0$ and assume for simplicity $(\eta_E/\eta_{||})$ constant in r

Integrating the continuity equation at null flow

$$[\upsilon_{||}+(\eta_E/\eta_{||})\upsilon_{ExB}]\,|_a^r=0\Rightarrow$$

$$\upsilon_\phi(r)=\frac{\{-(B_p/B_t)\upsilon_*^{neo}-(\eta_E/\eta_{||})[\upsilon_*(B/B_t)+\upsilon_*^{neo}]\}\,|_a^r}{\{1-(\eta_E/\eta_{||})(B_p/B_t)\}(r)}+\frac{\{1-(\eta_E/\eta_{||})(B_p/B_t)\}(a)}{\{1-(\eta_E/\eta_{||})(B_p/B_t)\}(r)}\upsilon_\phi(a)$$

If the edge rotation is small, the intrinsic toroidal rotation is diamagnetically scaled, i.e. driven by pressure and temperature gradients and proportional to rho-star.

Note even with $(\eta_E/\eta_{||})=0$: $\quad \upsilon_\phi(r)=\{-(B_p/B_t)\upsilon_*^{neo}\}\,|_a^r+\upsilon_\phi(a)$

- Assume $(\eta_\upsilon/a)\neq 0$ and $(\eta_E/\eta_{||})=0$, there is a similar solution:

$$\upsilon_\phi(r)=-(B_p/B_t)\upsilon_*^{neo}(r)+\{\upsilon_\phi+(B_p/B_t)\upsilon_*^{neo}\}(a)\exp\{-\textstyle\int_a^r(\eta_\upsilon/\eta_{||})dr'/a\}$$

- We don't really need the pinch effects $(\eta_E/\eta_{||})$ and (η_υ/a) to get intrinsic toroidal rotation, since radial flow is driven by $-\partial\upsilon_{||}/\partial r$ not $-\partial\upsilon_\phi/\partial r$

Heuristic: Diamagnetically scaled intrinsic toroidal rotation

- Getting the correct non-monotonic profile of $\upsilon_\phi(r)$ will require a very accurate transport model. Getting the finite $\upsilon_{||}$ curvature drift pinch effect in TGLF is straight-forward. Getting the ExB shear properly installed in the TGLF θ–dependent quasilinear mode function is non-trivial.

- However the diamagnetic scaling is testable: Assuming $\upsilon_\phi(a) \sim 0$

$$\upsilon_\phi(scale) \sim \upsilon_* \propto \rho_* c_s \sim c_s^2 / a / (eB/mc) \sim T/Ba$$

$$\tau_E \sim 3nTV/P \sim 3nT(\pi a^2 2\pi R\kappa)/P$$

$$\Rightarrow \upsilon_\phi(scale) \propto \tau_E (P/n)/(Ba^3 R\kappa)$$

- Using a collisionless-electrostatic-gyroBohm scaling

$$\tau_E \propto a^2 [B^2 a\kappa^2 / \hat{\chi}]^{2/5} (\kappa nR/P)^{3/5}$$

$$\hat{\chi}(GYRO) \propto q^2/\kappa \ \ \& \ \ I \propto a^2 B\kappa / Rq$$

$$\upsilon_\phi(scale) \propto a^2 [I^2 R^2 \kappa / a^3]^{2/5} (\kappa nR/P)^{3/5} (P/n)/(Ba^3 R\kappa)$$

$$\propto I^{4/5} B^{-1} (P/n)^{2/5} \kappa^0 R^{2/5} a^{-11/5}$$

- For $\upsilon_\phi(scale) \sim \upsilon_* \propto \rho_* c_s$, the shear rates $\propto \rho_* c_s / a$ will much smaller than high-n turbulent growth rates $\propto c_s / a$ in ITER. [May be helpful for stabilizing RWM?]

Heuristic: Edge source constraint

- While it appears the null flow profiles could have both co- and counter-current intrinsic rotation as a function of radius $\upsilon_\phi(r_1)<0;\ \upsilon_\phi(r_2)(>0)$ the edge source is only co-current.

- Since toroidal angular momentum is conserved $\int_0^a r'dr'nRM\upsilon_\phi(r')$ must be co-current.

- Ion orbit losses produce co-current momentum into as does the Debye shear Er ExB rotation.

- Hopefully the edge boundary condition $\upsilon_\phi(a)$ is "small" because we can at best put bounds on it:

$\upsilon_\phi^{\max}(a) = (B_t/B)\upsilon_\parallel^{\max}(a) - (B_p/B)\upsilon_\perp(a)$; $(B_t/B)>0$; $(B_p/B)>0$; $j_\phi<0$; $\upsilon_\parallel<0$ ->co
$\upsilon_\perp(a) = \upsilon_E(a) + \upsilon_*(a)$; $-\nabla_x P_i > 0$; $E_r(a) = -\nabla_x\phi(a) = -3\nabla_x T_e(a)/e > 0$; $\upsilon_\perp(a) > 0$ ->co

Empty loss cone gives $\upsilon_\parallel^{\max} \sim -\upsilon_{th}(a/R)/(2\sqrt{\pi}) \sim -0.1\upsilon_{th}$
and the $\upsilon_\perp(a)$ projection is much smaller.

In this discussion, it is important to remind that the source is taken to be outside $r=a$, i.e. $a<r<a+\rho_{banana}$. This likely means that $a=r_{ped}$ i. e. the top of the pedestal radius.

GYRO simulations verify the pinch effects

GA standard case with kinetic electrons: q=2,s=1, a/L_T=3, a/L_n=1, $\nu_* = 0$, $\beta = 0$
The particle pinch $D^{eff}/\chi^{eff}_{Ei} \sim -0.15$ has been "subtracted". $\gamma_p \equiv (r/a)\partial[(a/r)u_{\|}]/\partial r$

Prandtl Number

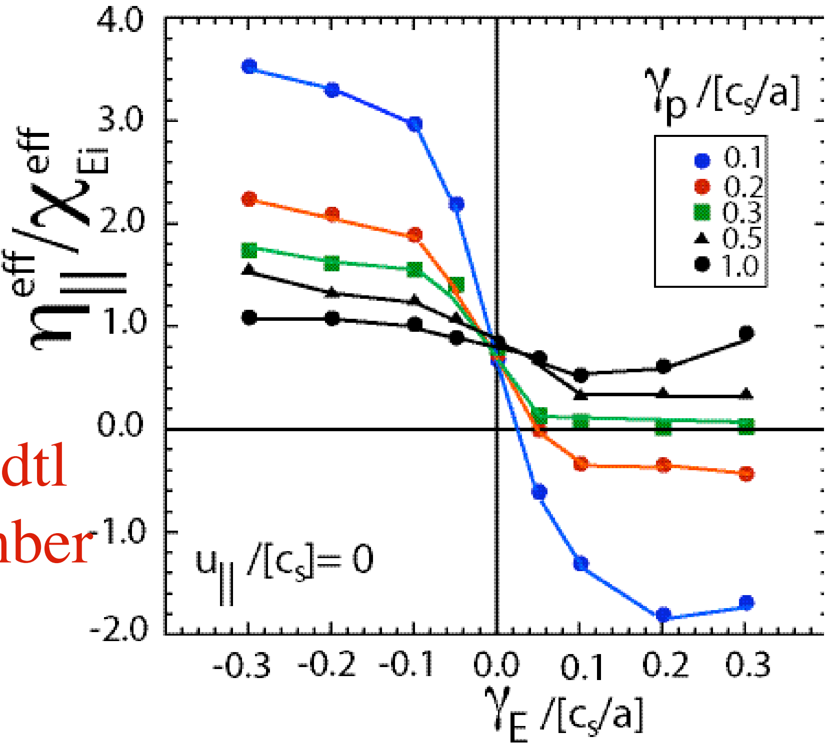

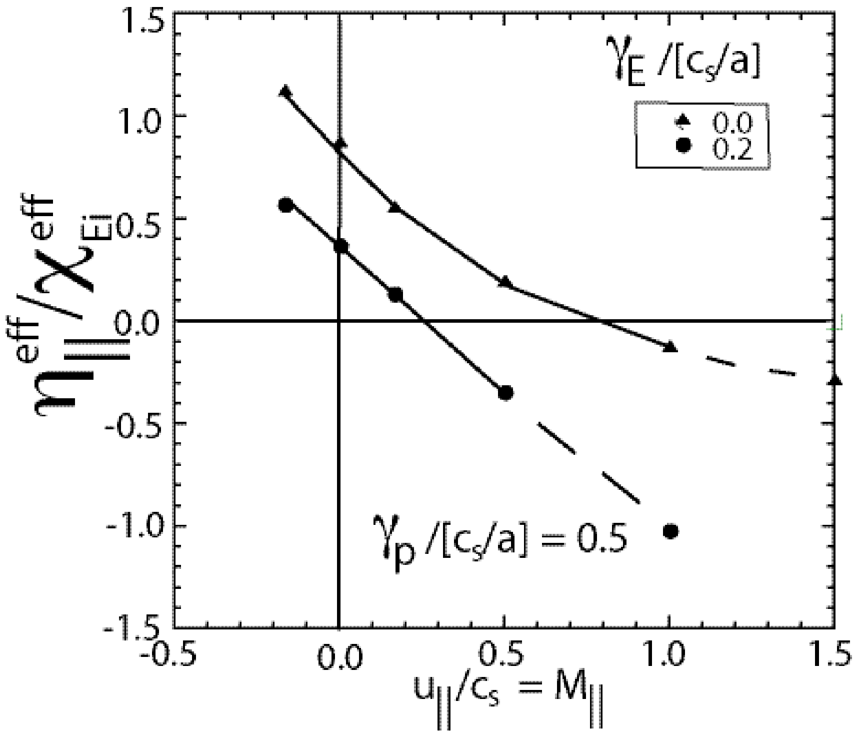

Note that the large parallel rotational shear states $\gamma_p \equiv -R\partial(u_{\|}/R)/\partial r \sim 1.0$ as in DIIID unbalance injection have the "normal" $\eta^{eff}_{\|}/\chi^{eff}_{Ei} \sim 0.8$ (previously reported in GYRO publications) are far from the pinched (or null) flow $\eta^{eff}_{\|}/\chi^{eff}_{Ei} \leq 0$

GYRO: ExB shear quench

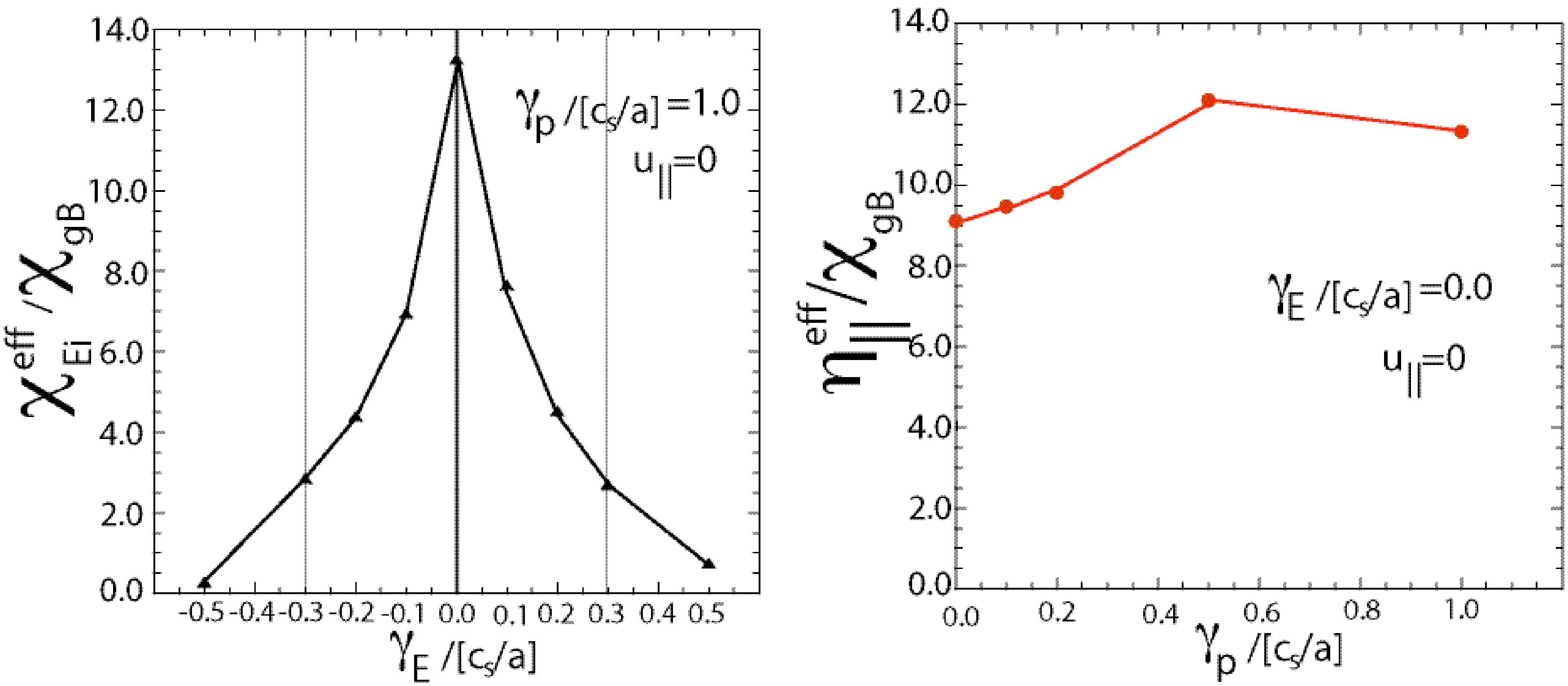

- ExB shear (independent of sign) has usual quench on all low-k transport channels.
- Momentum (and energy) diffusivity increases slightly with parallel velocity shear.

GYRO: GA-std case transport components

γ_p	γ_E	$M_\parallel$	$\eta_\parallel^{eff}$	$\eta_{\parallel z}^{eff}$	$\eta_{\parallel y}^{eff}$	χ_{Ei}^{eff}	χ_{Ee}^{eff}	D	$\eta_\parallel^{eff}/\chi_{Ei}^{eff}$	Δu_θ^{neo}
c_s/a	..	$u_\parallel/c_s$	$c_s a\rho_*^2$	..	..	..	..	..		$c_s\rho_*^2$
1.0	0.0	0.0	11.5	11.1	0.42	13.3	3.57	-1.97	0.86	+43
0.2	0.0	0.0	9.61	9.47	0.14	13.0	3.38	-2.10	0.74	+53
0.2	0.2	0.0	-1.29	0.15	-1.44	4.14	1.53	-0.87	-0.31	+19
0.2	0.0	0.4	-11.1	-10.2	-0.85	14.8	3.75	-2.35	-0.74	+48

- GA-std case: $R/a=3,\ r/a=0.5,\ q=2,\ \hat{s}=1,\ a/L_T=3,\ a/L_n=1,\ T_e/T_i=1,\ \nu_{ei}/[c_s/a]=0$
- $\Gamma_x^\phi/(Rm_i)-u_\phi\Gamma_x=-\eta_\parallel^{eff}\,\partial u_\parallel/\partial r=-\eta_{\parallel z}^{eff}\,\partial u_\parallel/\partial r-\eta_{\parallel y}^{eff}\,\partial u_\parallel/\partial r \qquad r\rightarrow x \qquad \perp\rightarrow y$
- $\Gamma_x^\phi=\left\langle|\nabla r|[\Pi_{xz}(B_t/B)R-\Pi_{xy}(B_p/B)R]\right\rangle$
- The Reynold stress $\Pi_{xy}\approx-(B/B_p)[n_i m_i]\eta_y^{\parallel}\gamma_p$ tend to diffuse poloidal rotation
- But the parallel stress Π_{zx} (magnetic pumping) tends to hold to neoclassical with a small turbulent shift $\Delta u_\theta^{neo}\sim 50c_s\rho_*^2$ about 10% of $u_*^{neo}\sim(-3.5\Rightarrow 5.1)c_s\rho_*$

Gyrokinetic formulation of toroidal angular momentum transport and poloidal rotation used in GYRO

G.M. Staebler, Phys. Plasmas (2004) 1064

- The toroidal angular momentum continuity equation is,
(ignoring small or explicitly zero magnetic flutter effects):

$$mn\partial\left\langle R\vec{u}\cdot\hat{\varepsilon}_{\phi}\right\rangle/\partial t+[V'(r)]^{-1}\partial_r V'(r)\{\Gamma^{\phi}+\Gamma^{\phi}_{conv}\}=\left\langle R\hat{\varepsilon}_{\phi}\cdot\vec{F}\right\rangle+\left\langle Rj_x B_p\right\rangle/c$$

$$\Gamma^{\phi}=\left\langle|\nabla r|[\Pi_{xz}(B_t/B)R+\Pi_{xy}(-B_p/B)R]\right\rangle=\Gamma^{\phi}_z+\Gamma^{\phi}_y$$

$$\Pi^{A}_{xz}\approx m\int d^3\upsilon[\upsilon_z(c\delta E_y/B]\delta f\ \sim\ \int d^3\upsilon\,[\sum_k(\delta\upsilon_{Ex})_{-k}m\upsilon_z J_0(k_\perp\rho_\perp)\delta g_k]\ \sim\ m\delta\upsilon_{Ex}\delta j^{i}_{z}/(en)$$

$$\Pi^{A}_{xy}\approx m\int d^3\upsilon[\upsilon_y(c\delta E_y/B)\delta f]\ \sim\ \int d^3\upsilon\,[\sum_k(\delta\upsilon_{Ex})_{-k}m\upsilon_\perp[ik_x/k_\perp]J_1(k_\perp\rho_\perp)\delta g_k]$$

$$\sim m\int d^3\upsilon\,[\sum_k(\delta\upsilon_{Ex})_{-k}\nabla_x(m\upsilon_\perp^2/2)(c/zeB)J_0(k_\perp\rho_\perp)\delta g_k]\ \sim\ m\delta\upsilon_{Ex}\delta j^{i}_{*y}/ze$$

The perpendicular stress Π^{A}_{xy} is significantly different from zero with ExB shear.

Gyrokinetic formulation of toroidal angular momentum transport and poloidal rotation used in GYRO (cont'd)

- The poloidal momentum balance is:

$$mn(1+2\bar{q}^2)\partial\left\langle B_p u_\theta\right\rangle/\partial t = -3\left\langle(\vec{b}\cdot\nabla B)^2\right\rangle\mu_1[(u_\theta - u_\theta^{neo} - \Delta u_\theta^{neo})/B_p + [B_t R/\left\langle R^2\right\rangle][\left\langle\vec{\nabla}\cdot\hat{\varepsilon}_x\Pi_{xy}(-B_p/B)R\right\rangle$$

$$-\left\langle\vec{\nabla}\cdot\hat{\varepsilon}_x\Pi_{xz}B\right\rangle + [B_t R/\left\langle R^2\right\rangle][\left\langle\hat{\varepsilon}_x\Pi_{xz}(B_t/B)R]\right\rangle]$$

$$+\left\langle BF_{||}\right\rangle - [B_t R/\left\langle R^2\right\rangle][\left\langle R\hat{\varepsilon}_\phi\cdot\vec{F}\right\rangle + \left\langle\vec{j}\cdot\nabla\psi\right\rangle/c]$$

(second line with Π_{xz} nearly cancels)

The "magnetic pumping" neoclassical viscosity dominates, dragging the poloidal velocity to the neoclassical value with a small turbulent shift (Staebler 2004):

$$K(\psi) = u_\theta/B_p \Rightarrow u_\theta^{neo}/B_p + \Delta u_\theta^{neo}/B_p \quad \text{where} \quad u_\theta^{neo} = [-1.17,\ 0.5,\ 1.7](a/L_T)\rho_* c_s$$

$$\Delta u_\theta^{neo} = B_p\left\langle(\vec{b}\cdot\vec{\nabla}B)\Delta_{zz}^A/2p\right\rangle/\left\langle(\vec{b}\cdot\vec{\nabla}B)^2\right\rangle \quad \text{where} \quad \Delta_{zz}^A = (4/3)\sum_s e_s \int d^3 v v_z \delta E_z \delta f_s = (4/3)\delta E_z \delta j_z$$

$$\Delta u_\theta^{neo} \sim O[\rho_* \hat{\chi}(a/L_T)](4/3)(R/a)[\sin(\theta)]\rho_* c_s$$

- For $\gamma_p = 0.2$ GYRO found (for GA-std) $\Delta u_\theta^{neo} \sim [50\rho_*,\ 19\rho_*]\rho_* c_s$ $\gamma_E = [0.0,\ 0.2]$

Gyrokinetic formulation of toroidal angular momentum transport and poloidal rotation used in GYRO (cont'd)

- The radial electric field $E_r = -|\nabla r|\partial\Phi/\partial r$ is given by :

$$\left\langle \vec{u}\cdot R\hat{\varepsilon}_\varphi \right\rangle = \left\langle R u_\varphi \right\rangle = \omega\left\langle R^2 \right\rangle + K\left\langle RB \right\rangle$$

where

$$\omega = -c[\partial\Phi/\partial\psi + (1/ne)\partial P/\partial\psi]$$
$$\partial_\psi = |\nabla r|/(B_p R)\partial_r$$
$$\partial\Phi/\partial\psi = -E_r/(B_p R)$$

- The ion "omega-star" and "omega-drift" terms for a parallel drifted Maxwellian

$$\partial\delta f/\partial t = ...-\{(\partial n_0/\partial r)/n_0 + [(m/2T_0)(\upsilon_\perp^2 + \upsilon_{||}'^2) - 3/2](\partial T_0/\partial r)/T_0$$
$$+2(m/2T_0)\upsilon_{||}'[R_0\partial(\left\langle u_{||}\right\rangle/R_0)/\partial r]\}\nabla r\cdot\hat{b}\times\nabla\left\langle \delta\phi - \upsilon_{||}\delta A_{||}\right\rangle F_0$$

$$\partial\delta f/\partial t + (c/B)\hat{b}\times[m(\upsilon_{||}'^2 + 2\left\langle u_{||}\right\rangle\upsilon'_{||})\hat{b}\cdot\vec{\nabla}\hat{b} + m\upsilon_\perp^2/2\vec{\nabla}B/B]\cdot\nabla\delta f + ... = ...$$

where $\gamma_p \equiv -R_0\partial[\left\langle u_{||}\right\rangle/R_0]/\partial r$ and $\upsilon_{||}'(\theta) = \upsilon_{th}\sqrt{\hat{\varepsilon}(1-\lambda B(\theta)} = \upsilon_{||} - u_{||}$

Summary: Momentum transport

- Intrinsic (or spontaneous) toroidal rotation driven by pressure and ion temperature gradients has been long predicted from the ExB shear pinch of toroidal momentum transport (Dominquez and Staebler 1993 & Staebler et al 2001).

- An additional finite parallel velocity - curvature pinch effect has been proposed (Peeters, Angioni, Strinzi 2007)

- GYRO has confirmed both pinch effects can result in a "null" radial flow of toroidal momentum $\eta_{\|}^{eff}/\chi_{Ei}^{eff} \sim 0$ at low parallel velocity shear whereas the normal $\eta_{\|}^{eff}/\chi_{Ei}^{eff} \sim 0.8$ obtains at high parallel velocity shear.

- If $\upsilon_{\phi}(a) << Max[\upsilon_{\phi}(r)]$ the intrinsic toroidal rotation with "null" radial flow will have a diamagnetic scaling $\upsilon_{\phi}(scale) \sim \upsilon_{*} \propto \rho_{*} c_{s}$ leading to ExB shear rates $\propto \rho_{*} c_{s}/a$ much smaller than high-n turbulent growth rates $\propto c_{s}/a$ in ITER.

- The edge source constrains the total intrinsic toroidal angular momentum to be co-current, but we can not predict the size of $\upsilon_{\phi}(a)$ without the source details.

- Accurately predicting the (often) non-monotonic radial profile of the intrinsic toroidal rotation will be a challenge for theory based transport code models.

- GYRO has shown the turbulent shift from neoclassical poloidal rotation is small.

Turbulent energy exchange

- Long history, comedy of errors, and (maybe ?) much to do about little.
- Can't define turbulent heating H without defining energy flux Q

$$\partial W/\partial t + \nabla\cdot[\vec{Q} + ..] = H + \ldots$$

- History

_Manheimer, Ott, and Tang (1977): exchange $H = -e[\partial\delta n/\partial t]\delta\phi$ $Q_x = q_x + 5/2\Gamma_x T$

_Waltz, Staebler, et al (GLF23 1997): exchange $H = -e[\partial\delta n/\partial t]\delta\phi$ $Q_x = q_x + 3/2\Gamma_x T$

_Hinton and Waltz (2006): heating $H = \delta j_{||}\delta E_{||}^{\phi} + \delta\vec{j}_{d\perp}\cdot\delta\vec{E}_{\perp}^{\phi} + \ldots$ $Q_x = q_x + 3/2\Gamma_x T$

_ G.G. Howes, S.C. Cowley,W. Dorland. G.W. Hammett, et al
astrophysics & heating of nebulae $H = \delta\vec{j}\cdot\delta\vec{E} = -\nabla\cdot\vec{F}_{em}$ $Q \sim 0$ $(ignored)$

Turbulent energy exchange (cont'd)

- Early tokamak papers had incorrect derivations setting $\{\langle \nabla\cdot(e\delta\vec{\Gamma}\delta\phi)\rangle^S\}^{xt} \to 0$

- Hinton & Waltz pointed out the that $\delta j_{\|}\delta E_{\|}^{\phi} + \delta\vec{j}_{d\perp}\cdot\delta\vec{E}_{\perp}^{\phi}$ is the "parallel nonlinearity". Took $\delta j_{\|}\delta E_{\|}^{\phi}$ to be heating, but mistook $\delta\vec{j}_{d\perp}\cdot\delta\vec{E}_{\perp}^{\phi}$ to be heating instead of cooling (simple sign error) ....opens way for $\delta j_{\|}\delta E_{\|}^{\phi} + \delta\vec{j}_{d\perp}\cdot\delta\vec{E}_{\perp}^{\phi}$ to be heating or cooling, hence possible electron-ion exchange

- Why can the PNL be dropped from delta-f gyrokinetic simulations?

$$\partial\delta w/\partial t + \nabla\cdot[\delta\vec{v}_E\delta w] + \ldots = \delta j_{\|}\delta E_{\|}^{\phi} + \delta\vec{j}_{d\perp}\cdot\delta\vec{E}_{\perp}^{\phi} \quad + \ldots \qquad \delta w = 3/2[n_0\delta T + T_0\delta n]$$

$$O(\rho_*) + O(1/\rho_*)O(\rho_*^2) + \ldots = O(\rho_*^2)$$

- We can show the *local radial average* (&flux-surface&time ave)

$$\{\langle \delta j_{\|}\delta E_{\|}^{\phi} + \delta\vec{j}_{d\perp}\cdot\delta\vec{E}_{\perp}^{\phi}\rangle^S\}^{xt} \equiv \{-\langle e[\partial\delta n/\partial t]\delta\phi\rangle^S\}^{xt}$$

which is clearly an exchange by quasi-neutrality $\quad -e\delta n_e + e\delta n_i = 0$

Turbulent energy exchange (cont'd)

- **Proof:** $\{\langle \delta j_{\|} \cdot \delta E_{\|} \rangle^{S} + \langle \delta \vec{j}_{d} \cdot \delta \vec{E}_{\perp} \rangle^{S} \}^{xt} = -\{\langle eD\delta n/Dt\delta\varphi \rangle^{S}\}^{xt}$

$$- e\langle \delta\varphi D\delta n/Dt \rangle = e^{2}\sum_{k} \delta\varphi_{-k} D[n_{0}\delta\varphi_{k}/Dt] - e\int dv^{3}\delta\varphi D J_{0}\delta g/Dt] = -e\int dv^{3}\langle\delta\varphi\rangle D\delta g/Dt$$

- **GK eq:** $-D\delta g_{k}/Dt = [\delta\vec{v}_{E}\cdot\vec{\nabla}_{\perp}\delta g]_{k} + i\omega_{*k}(e\langle\delta\varphi_{k}\rangle/T)F_{0}$

$$-(eF_{0}/T)\partial\langle\delta\varphi_{k}\rangle/\partial t + v_{\|}\vec{b}\cdot\nabla\delta g_{k} + \vec{v}_{d}\cdot\vec{\nabla}_{\perp}\delta g$$

- **mult. by** $\langle\delta\varphi_{-k}\rangle$ **followed by** $\{\ \}^{xt}$ $\quad \langle\ \rangle^{S} \Rightarrow \Sigma_{k}$

$$\{\langle \sum_{k}\langle\delta\varphi\rangle_{-k}[\delta\vec{v}_{E}\cdot\vec{\nabla}_{\perp}\delta g]_{k}\rangle^{S}\}^{t} = \{\langle \sum_{k}\langle\delta\varphi\rangle_{-k}[c\vec{b}\times\vec{\nabla}_{\perp}\langle\delta\varphi\rangle/B\cdot\vec{\nabla}_{\perp}\delta g]_{k}\rangle^{S}\}^{t} = 0$$

$$\{\langle \int dv^{3}\sum_{k}\langle\delta\varphi\rangle_{-k} i\omega_{*k} e\langle\delta\varphi\rangle_{k}/TF_{0}\rangle^{S}\}^{t} = 0$$

$$\{\langle \int dv^{3}\sum_{k}\langle\delta\varphi\rangle_{-k} e/TF_{0}\partial\langle\delta\varphi\rangle_{k}/\partial t\rangle^{S}\}^{t} = \{en_{0}/T\partial\langle\partial[\sum_{k}|\langle\delta\varphi\rangle|^{2}k]/2\rangle^{S}/\partial t\}^{t} = 0$$

$$\{\langle \int dv^{3}\sum_{k}\langle\delta\varphi\rangle_{-k} v_{\|}\vec{b}\cdot\nabla\delta g_{k}\rangle^{S}\}^{t} = \{\sum_{k}\langle[\delta E_{\|}]_{-k}\int dv^{3} v_{\|}\langle\delta g_{k}\rangle\rangle^{S}\}^{t} = \{\langle\delta j_{\|}\cdot\delta E_{\|}\rangle^{S}\}^{xt}$$

$$\{\langle \sum_{k}\langle\delta\varphi\rangle_{-k}[\vec{v}_{d}\cdot\vec{\nabla}_{\perp}\delta g]_{k}\rangle^{S}\}^{t} = \{\langle \sum_{k}[\delta\vec{E}_{\perp}]_{-k}[\cdot\vec{v}_{d}\langle\delta g\rangle]_{k}\rangle^{S}\}^{t} = \{\langle\delta\vec{j}_{d}\cdot\delta\vec{E}_{\perp}\rangle^{S}\}^{xt}$$

Turbulent energy exchange (cont'd)

- **Exchange form of energy continuity equation:**

$$\frac{\partial W}{\partial t}+\vec{\nabla}\cdot\left(\hat{b}Q_{||}+\vec{Q}^{nc}+\vec{Q}^{D}\right)=e\left[\Gamma_{||}E_{||}+\left(\vec{\Gamma}^{nc}+\vec{\Gamma}_{\perp}^{D}\right)\cdot\vec{E}\right]+\dot{W}_{C}+e\left(\delta\Gamma_{||}\delta E_{||}+\delta\vec{\Gamma}_{\perp}\cdot\delta\vec{E}_{\perp}\right)$$

$$e\,\partial\delta n/\partial t+e\vec{\nabla}\cdot\delta\Gamma=0\Rightarrow$$

$$e\delta\varphi\partial\delta n/\partial t+\vec{\nabla}\cdot(e\delta\vec{\Gamma}\delta\varphi)=+e\delta\vec{\Gamma}\cdot\vec{\nabla}\delta\varphi=-e\delta\vec{\Gamma}\cdot\delta\vec{E}$$

$$\frac{\partial W}{\partial t}+\vec{\nabla}\cdot\left(\hat{b}Q_{||}+\vec{Q}^{nc}+\vec{Q}^{D}+e\delta\varphi\delta\vec{\Gamma}\right)=e\left[\Gamma_{||}E_{||}+\left(\vec{\Gamma}^{nc}\right)\cdot\vec{E}\right]+\dot{W}_{C}-e\left(\delta\varphi D\delta n/Dt\right)$$

$$\left\langle\vec{\nabla}\cdot Q\right\rangle^{S}=1/V'(r)\partial[V'(r)\left\langle|\nabla r|Q_{x}\right\rangle^{S}]/\partial r$$

$$Q_{x}=Q_{x}^{nc}+Q_{x}^{D}+e\delta\varphi\delta\Gamma_{x}=Q_{x}^{nc}+Q_{x}^{G}+[Q_{x}^{X}+e\delta\varphi\delta\Gamma_{x}]$$

But $\{\left\langle Q_{x}^{X}+e\delta\varphi\delta\Gamma_{x}\right\rangle^{S}\}^{xt}=0$

- **There is addition magnetic energy flux plus possible heating:** $\delta j_{||}[\partial\delta A_{||}/\partial t]/c$
Although $\{\left\langle\delta j_{||}[\partial\delta A_{||}/\partial t]/c\right\rangle^{S}\}^{xt}=0$ **adding the species.**

Turbulent energy exchange (cont'd)

- Proof: $\{\left\langle Q_x^X + e\delta\varphi\delta\Gamma_x \right\rangle^S\}^{xt} = 0$

(1) $(c/B)[m\int dv^3 v_y \delta f(v_x \delta E_x] \Rightarrow (cm/B)\sum_k [\int dv^3 v_\perp^2 \{(k_y k_x/k_\perp^2) J_2(ik_x)\}\delta g]_k [\delta\varphi]_{-k}$

(2) $(c/B)[m\int dv^3 v_y \delta f(v_y \delta E_y] \Rightarrow$

$$(cm/B)\sum_k [\int dv^3 v_\perp^2 \{(k_y k_y/k_\perp^2) J_2 ik_y + (J_0 - J_2) ik_y/2\}\delta g]_k [\delta\varphi]_{-k}$$

(3) $(c/B)[m\int dv^3 v_y \delta f(v_z \delta E_z)] \Rightarrow (mc/B)[\int dv^3 v_z v_\perp \{(ik_x/k_\perp) J_1(z)\}\delta g]_{-k} [\delta E_z]_{-k}$

(4) $e\delta\varphi\delta\Gamma_x = e[\int dv^3 v_x \delta f]\delta\varphi \Rightarrow (cm/B)\sum_k [\int dv^3 v_\perp^2 \{-ik_y J_1(z)/z\}\delta g]_k [\delta\varphi]_{-k}$

(1)+(2)+(4) =0 using $J_1(z)/z = (J_0(z) + J_2(z))/2$

$\{\} = \{-ik_y(J_0(z) + J_2(z))/2\} + \{(k_y k_x/k_\perp^2) J_2(ik_x)\} + \{(k_y k_y/k_\perp^2) J_2 ik_y + (J_0 - J_2) ik_y/2\} = 0$

(3) is smaller by $O(\rho_*)$

GYRO cyclic flux tube simulations of turbulent heating

ion mode: a/LT=3 a/Ln=1 otherwise GA-std case

*	$\{\langle \delta j_{\parallel} \delta E_{\parallel} \rangle^{S}\}^{xt}$	$\{\langle \delta \vec{j}_d \cdot \delta \vec{E}_{\perp} \rangle^{S}\}^{xt}$	H	$\chi \otimes (a/L_T)$	$D \otimes (a/L_n)$
electron	5.0	-1.3	+4.3 ± 2.0	3.1 x 3= 9.3	-1.9x1=-1.9
ion	9.0	-12.4	-3.4 ± 2.8	11.1x3=33.3	-1.9x1=-1.9

electron mode: a/LT=1 a/Ln=3

electron	12.18	-12.43	-0.26 ±1.25	30.5x1=30.5	5.7x3=17.1
ion	9.3	-8.8	+0.44 ±2.30	26.1x1=26.1	5.7x3=17.1

mixed mode: a/LT=2 a/Ln=2

electron	6.2	-7.6	-1.5 ± 1.6	13.2x2=26.4	4.7x2=9.4
ion	10.1	-8.2	+1.9 ± 2.9	13.0x2=26.0	4.7x2=9.4

* For ion mode case: a/LTi=3 a/LTe=2 a/Ln=1 $D \otimes (a/L_n) \sim 0$

$H_e(H_i) = 6.3 \pm 2.4(-5.4 \pm 3.1)$ $\chi_{Ee} \otimes a/L_T = 6.6(\chi_{Ei} \otimes a/L_T = 39.6)$

GYRO global simulations of turbulent heating

DIII-D L-mode #101391 Bt=2.1T

$$H = \{ \langle \delta j_{||} \delta E_{||} + \delta \vec{j}_{d\perp} \cdot \delta \vec{E}_{\perp} \rangle^{S} \}^{t}$$

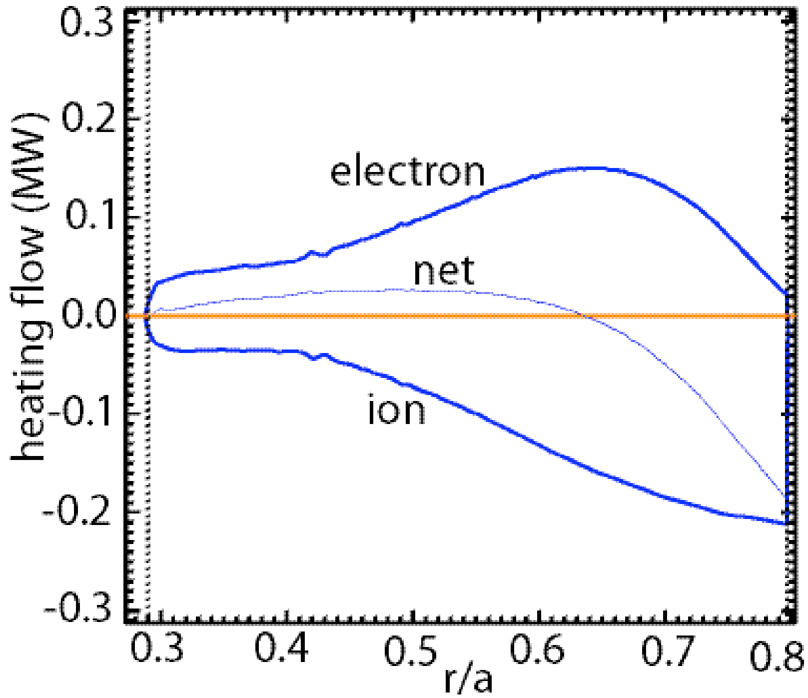

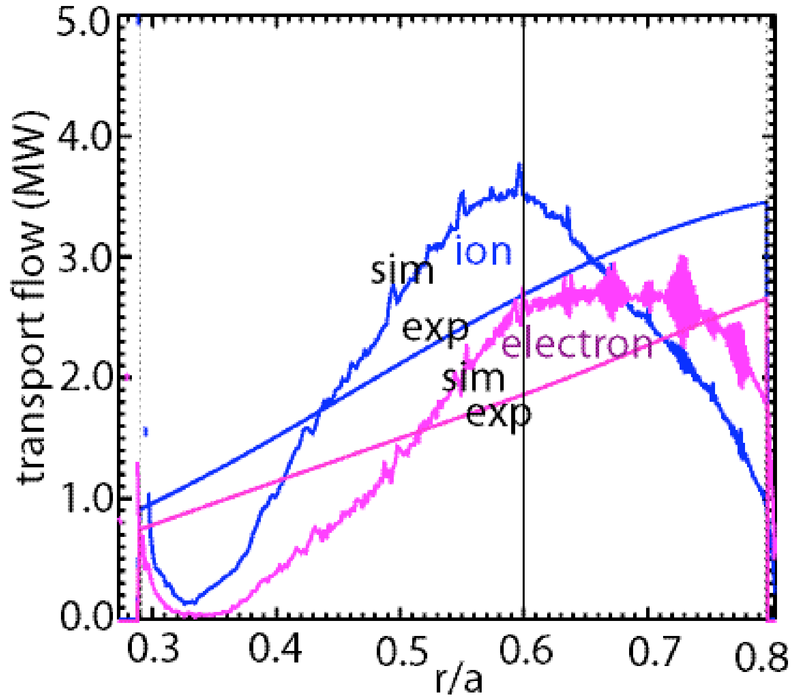

- At r/a ~0.6 exchange flow is about 5% transport flow
- For r/a > 0.65 exact exchange appear to breakdown because there is no local radial averaging
- $\delta j_{||} \delta E_{||} + \delta \vec{j}_{d\perp} \cdot \delta \vec{E}_{\perp}$ form consistent with conservative drift kinetic equations with no radial average.

Summary: Gyrokinetic turbulent energy exchange

- Must define gyrokinetic turbulent heating with respect to gyrokinetic energy flow.
- $\delta j_{||}\delta E_{||} + \delta\vec{j}_{d\perp}\cdot\delta\vec{E}_{\perp}$ form consistent with drift-kinetic equation which requires no local averaging, and is actually the same as the "parallel nonlinearity"
- The local radial average of turbulent heating is an electron-ion energy exchange.
- The exchange electrons heated (cooled) for ion (electron) modes
- The integrated heating (cooling) flows appear to the less than 10% of transport flows.

GYRO references

[Candy 2003a] J. Candy and R.E. Waltz, “An Eulerian Gyrokinetic-Maxwell Solver,” J. Comput. Phys. **186**, 545 (2003).

[Candy 2003b] J. Candy and R.E. Waltz, “Anomalous Transport in the DIII-D Tokamak Matched by Supercomputer Simulation,” Phys. Rev. Lett. **91**, 045001-1 (2003).

[Candy 2004a] J. Candy, R.E. Waltz, and W. Dorland, “The Local Limit of Global Gyrokinetic Simulations,” Phys. Plasmas **11**, L25 (2004).

[Candy 2004b] J. Candy, M.N. Rosenbluth, and R.E. Waltz, "Smoothness of turbulent transport across a minimum-q surface", Phys. Plasmas **11**, 1879 (2004).

[Candy 2005] J. Candy, “Beta Scaling of Transport in Microturbulence Simulations,” Phys. Plasmas **12**, 072307 (2005).

[Candy 2006a] J. Candy and R.E. Waltz, “Velocity-Space Resolution, Entropy Production, and Upwind Dissipation in Eulerian Gyrokinetic Simulations,” Phys. Plasmas **13**, 032310 (2006).

[Candy 2006b] J. Candy, R.E. Waltz, S.E. Parker, and Y. Chen, “Relevance of the Parallel Nonlinearity in Gyrokinetic Simulations of Tokamak Plasmas,” Phys. Plasmas **13**, 074501 (2006).

[Candy 2006c] J. Candy and R.E. Waltz, “Coupled ITG/TEM-ETG Gyrokinetic Simulation,” Proc. 21st IAEA Fusion Energy Conf., Chengdu, China, 2006, Paper TH/2-1.

[Candy 2007] J. Candy, R.E. Waltz, M. Fahey, and C. Holland, “The Effect of Ion-Scale Dynamics on Electron-Temperature-Gradient Turbulence,” Plas. Phys. Control. Fusion **49** 1209 (2007)

GYRO references

[Estrada-Mila 2005] C. Estrada-Mila, J. Candy, R.E. Waltz, “Gyrokinetic Simulations of Ion and Impurity Transport,” Phys. Plasmas **12**, 022305 (2005).

[Estrada-Mila 2006a] C. Estrada-Mila, J. Candy, and R.E. Waltz, “Density Peaking and Turbulent Pinch in DIII-D Discharges,” Phys. Plasmas **13**, 074505 (2006).

[Estrada-Mila 2006b] C. Estrada-Mila, J. Candy, and R.E. Waltz, “Turbulent Transport of Alpha Particles and Helium Ash in Reactor Plasmas,” Phys. Plasmas **13**, 112303 (2006).

[Hinton 2004] F.L. Hinton, R.E. Waltz, and J. Candy, “Effects of Electromagnetic Turbulence in the Neoclassical Ohm’s Law,” Phys. Plasmas **11**, 2594 (2004).

[Hinton 2006] F.L. Hinton, and R.E. Waltz, “Gyrokinetic Turbulent Heating,” Phys. Plasmas **13**, 102301 (2006).

[Kinsey 2005] J.E. Kinsey, R.E. Waltz, J. Candy, “Nonlinear gyrokinetic simulations of ExB shear quenching of transport", Phys. Plasmas **12**, 062302 (2005)

[Kinsey 2006] J.E. Kinsey, R.E. Waltz, and J. Candy, “The Effects of Safety Factor and Magnetic Shear on Turbulent Transport in Nonlinear Gyrokinetic Simulations,” Phys. Plasmas **13**, 022305 (2006).

[Kinsey 2007] J.E. Kinsey, R.E. Waltz, J. Candy, “The Effect of Plasma Shaping on Turbulent Transport and ExB Shear Quenching in Nonlinear Gyrokinetic Simulations,” accepted for publication in Phys. Plasmas,

[Staebler 2005] G.M. Staebler, J.E. Kinsey, and R.E. Waltz, “Gyro-Landau Fluid Equations for Trapped and Passing Particles,” Phys. Plasmas **12**, 102508 (2005).

GYRO references

[Staebler 2007] G.M. Staebler, J.E. Kinsey and R.E. Waltz, "A Theory Based Transport Model with Comprehensive Physics," APS06 Issue Phys. Plasmas **14**, 0055909 (2007)

[Waltz 2002] R.E. Waltz, J. Candy, and M.N. Rosenbluth, "Gyrokinetic Turbulence Simulation of Profile Shear Stabilization and Broken Gyrobohm Scaling," Phys. Plasmas **9**, 1938 (2002).

[Waltz 2005a] R.E. Waltz, J. Candy, F.L. Hinton, C. Estrada-Mila, J.E. Kinsey, "Advances in Comprehensive Gyro-kinetic Simulations of Transport in Tokamaks," Nucl. Fusion **45**, 741 (2005).

[Waltz 2005b] R.E. Waltz, J. Candy, "Heuristic Theory of Nonlocally Broken Gyro-Bohm Scaling," Phys. Plasmas **12**, 072303 (2005).

[Waltz 2005c] R.E. Waltz, "ρ^* Scaling of Physically Realistic Gyrokinetic Simulations of Transport in DIII-D," Fusion Sci. Technol. **48**, 1051 (2005).

[Waltz 2006a] R.E. Waltz, J. Candy, and C.C. Petty, "Projected Profile Similarity in Bohm and GyroBohm Scaled DIII-D L- and H-Modes," Phys. Plasmas **13**, 072304 (2006).

[Waltz 2006b] R.E. Waltz, M.E. Austin, K.H. Burrell, and J. Candy, "Gyrokinetic Simulations of Off-Axis Minimum-q Profile Corrugations," Phys. Plasmas **13**, 052301 (2006).

[Waltz 2007a] R.E. Waltz, J. Candy, and M. Fahey, "Coupled Ion Temperature Gradient and Trapped Electron Mode to Electron Temperature Gradient Mode Gyrokinetic Simulations," APS06 Issue Phys. Plasmas **14**, 0056116 (2007)

[Waltz 2007b] R.E. Waltz, G. M. Staebler, J. Candy, and F. Hinton, "Gyrokinetic Theory and Simulation of Toroidal Angular Momentum Transport", submitted to Phys. Plasmas

[Waltz 2007c] R.E. Waltz, G. M. Staebler, and J. Candy, "Gyrokinetic Theory and Simulation of Turbulent Energy Exchange", to be submitted Phys. Plasmas